

## Capteur communicant par rétro-modulation dans la bande 5G *Backscattered communication in the 5G band for ultra-low power sensors*

*Neel Samat<sup>1</sup>, Arnaud Vena<sup>2</sup>, Brice Sorli<sup>3</sup>, Jean Podlecki<sup>4</sup>*

<sup>1</sup>*IES, University of Montpellier/CNRS, samatneel@gmail.com*

<sup>2</sup>*IES, University of Montpellier/CNRS, arnaud.vena@umontpellier.fr*

<sup>3</sup>*IES, University of Montpellier/CNRS, brice.sorli@umontpellier.fr*

<sup>4</sup>*IES, University of Montpellier/CNRS, jean.podlecki@umontpellier.fr*

*Mots clés (en français et en anglais) : Rétro-modulation, 5G, capteurs sans fils, radio-logicielle, Backscattering, 5G, wireless, sensor, software defined radio.*

### Résumé/Abstract

Dans cet article nous présentons une nouvelle architecture de capteurs sans fil alimenté par une cellule photovoltaïque de taille réduite. Le dispositif communique en sans-fil via le principe de rétro-modulation sur une bande de fréquence relativement large incluant la bande 5G (3.4GHz – 3.8GHz). Le dispositif réalisé est capable de transmettre une information de température et d’humidité à plusieurs mètres dans un environnement indoor en consommant très peu d’énergie pouvant être fournie par une petite cellule solaire positionnée proche d’une fenêtre pour capter le rayonnement solaire. Le capteur sans fil a été réalisé et testé à l’aide d’un équipement de radio logicielle (USRP).

We report the study of a novel ultra-low power wireless sensor node with self-energy harvesting based on a limited size photovoltaic cell. This device communicates wirelessly based on backscattering principle over a wide frequency band compatible with 5G (3.4GHz – 3.8GHz). The realized device is able to communicate both temperature and humidity over a range of several meters in indoor environment while consuming few energy that can be supplied by a small photovoltaic cell located close to a window to catch the sun light. The wireless sensor was realized and tested with a help of a software defined radio based equipment (USRP).

### 1 Introduction

The principle of wireless communication by means of reflected power is studied and utilized since the second world war. It has been theorized first by Stockman [1] and later applied for the well know RFID technology [2][3] specially in the UHF band (840 MHz – 960 MHz). Since few years, backscattering communication principle is subject to a growing interest for the IoT (internet of things) [4] because it allows communicating between a base station and remote devices with few energy to compare with others conventional wireless communication systems [4][5][6][7][8]. It is particularly interesting to focus this study in the 3.4GHz-3.8GHz band because in the novel paradigm proposed with the 5G, base stations are supposed to be ubiquitous so that radio devices will likely find a 5G signal surrounding them. For the remote node, the communication section requires only a switching component to connect the antenna to two different loads (see Fig. 1).

This paper presents a novel ultra-low power wireless sensor node operating in 5G with self-energy harvesting based on a limited size photovoltaic cell. The structure of this paper is as follows. Section 2 provides the theory and design of the proposed novel backscattered based transponder. Section 3 explains the detection system based on a software defined radio operating in 5G. Section 4 presents measurements results before concluding.

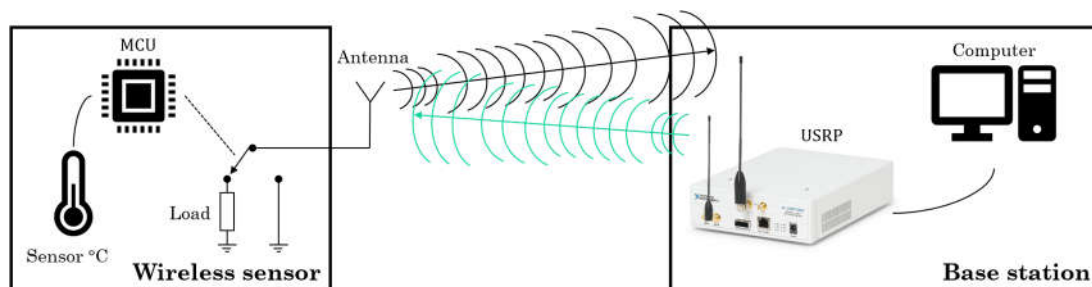


*Figure 1 – Backscattering communication principle*

## 2 Theory and design of an ultra-low power backscatter communication based transponder

The studied remote node is based on a bistatic backscatter communication system (BBCS). In the BBCS architecture, there is an RF source (carrier emitter), a backscatter receiver and a backscatter transmitter. The RF source generates continuous carrier signal that will serve as a support for the backscatter based communication from the remote transponder to the base station. Unlike UHF passive RFID, the remote transponder is not remotely powered by the EM field of the base station, but it uses an external power supply; hence, the distance of communication can be increased. Besides, the coding and modulation scheme is open and not ruled by the EPC Gen2 standard.

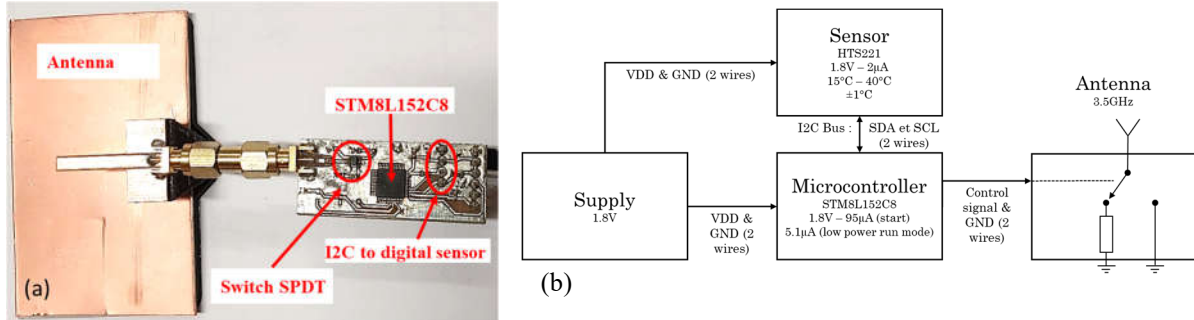


Figure 2: (a) Realized remote low power node (b) Circuit diagram of the remote low power node

The transponder is based on an 8-bit ultra-low power microcontroller (STM8L152C8) connected to a SPDT switch for antenna load modulation as shown in Fig. 2 (a) and (b). For the sake of demonstration, we connected the microcontroller to a low power digital sensor (HTS221) through an I2C connection. The microcontroller (STM8L152C8) is the key of the power consumption. Indeed, as shown in the Fig. 3 (a), the “main” function uses several functions such the “Low Power Run Mode” which allows to set low frequency clock and to copy the program in the RAM. The data acquisition from the sensor (HTS221) and the data transmission is executed from the RAM, that helps in saving power. Indeed, current consumed is equal to 1mA with all peripherals switched on and with the program executed from the Flash memory, whereas it is below 10 $\mu$ A under 1.8V when executed in RAM in “low power run” mode with all peripherals switched off.

In this study we decided to modulate the incoming CW of the base station by switching a load between off state and 50 $\Omega$ . This switching is driven by a low frequency subcarrier according to a frequency shift-keying (FSK) modulation illustrated in Fig. 3 (b), (c), (d) that show the serialized 8-bits binary data, the FSK modulated subcarrier that command the SPDT switch, and the reflected EM signal modulated by the subcarrier signal, respectively. As shown in Fig. 3 (b) and (c), a binary ‘0’ generates a subcarrier at  $f_{sc1}=5$ kHz, whereas a ‘1’ is coded by a subcarrier at  $f_{sc2}=10$ kHz. As a result, we can observe in the spectrum (see Fig. 6) the apparition of two sidebands around the carrier frequency for which the frequency is modulated between two values  $f_{sc1}=5$ kHz and  $f_{sc2}=10$ kHz to encode a binary value ‘0’ and ‘1’, respectively.

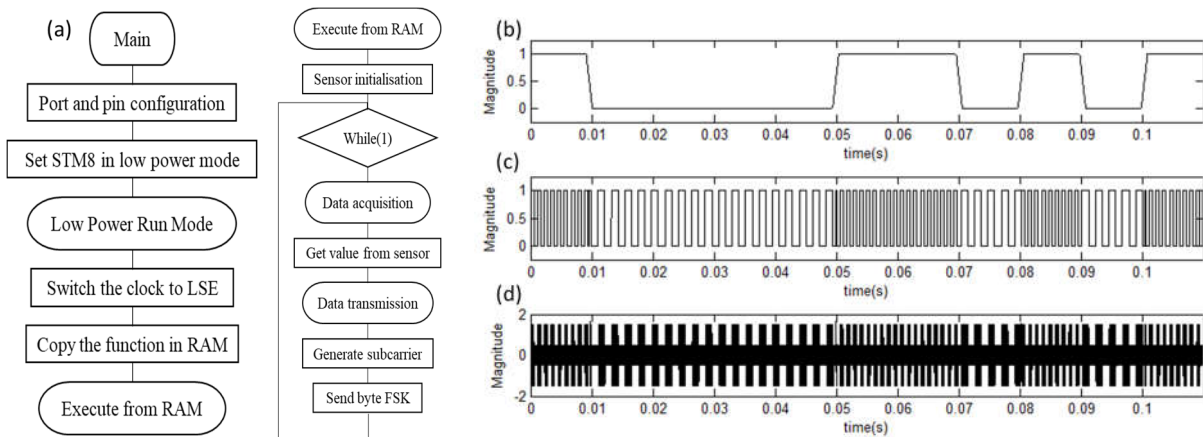


Figure 3 – (a) Flowchart of the main function and the function run in RAM (b) Serialized 8-bits binary data (c) FSK modulated subcarrier according to the 8-bits binary data (d) Reflected EM signal modulated by the subcarrier

The antenna shown in Fig. 2 (a) was design on FR-4 substrate ( $\epsilon_r=4.5$ ) to operate within the range 3.4GHz to 3.8GHz. It is based on a monopole antenna fed by a coaxial termination via a  $50\Omega$  CPW line. In order to increase the gain to an acceptable value, a reflector is inserted back of the monopole antenna at distance of 15mm. The overall dimensions of the reflector are 50mmx80mm and the monopole antenna has a length of 18.35mm. As shown in Fig. 4 (a) and (b) the simulated results of the antenna show a -10dB operating bandwidth between 3.41GHz and 3.88GHz and a gain of 6.22dBi at 3.6GHz. This antenna is directly connected to the SPDT switch of the transponder board via an SMA connector (see Fig 2 (a)).

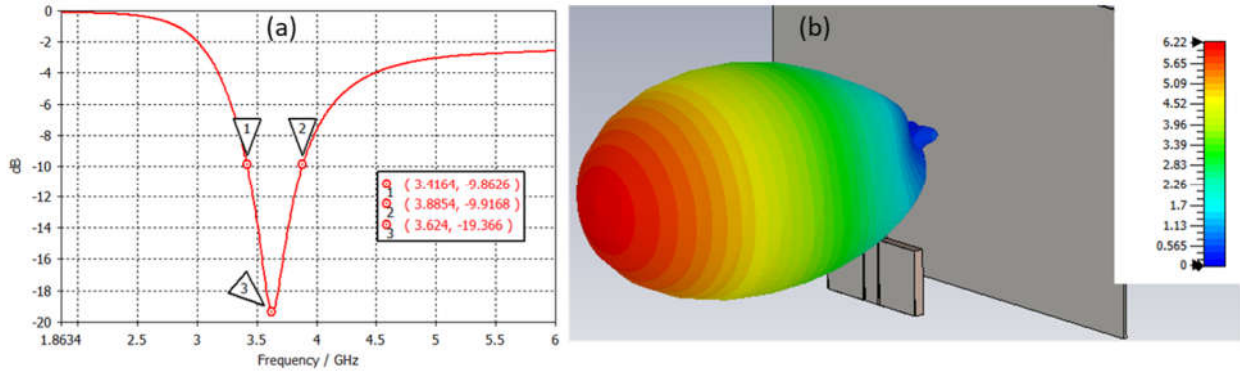


Figure 4 –(a) Simulated return loss of the designed 5G antenna (b) Radiation pattern (IEEE Gain) in dBi

## 2.1 Design of the 5G backscattering communication based base station

At the receiver side we used an USRP NI-2901 from National Instrument that is a software defined radio operating within the frequency range 70MHz to 6GHz with a maximum sampling rate of 61.44Ms/s. We developed a control software based on GnuRadio libraries to manage one TX channel and one RX channel. As shown in the architecture diagram of the software in Fig. 5, the TX channel is used to generate an unmodulated single tone carrier signal in the frequency range 3.4GHz to 3.8GHz.

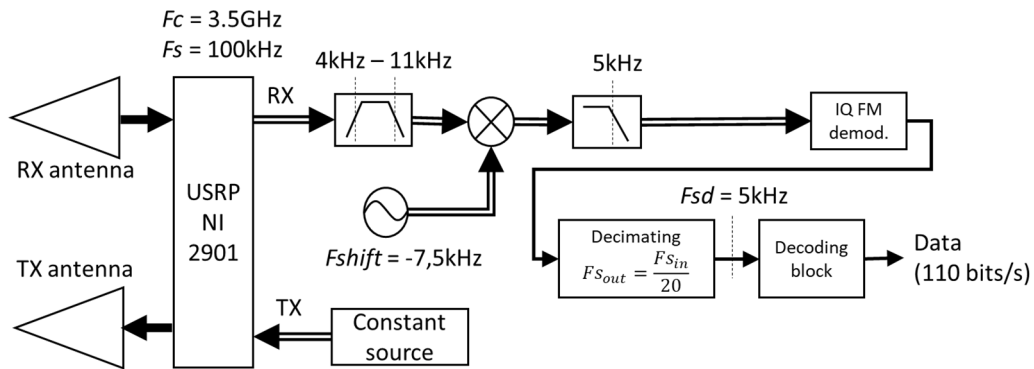


Figure 5 – Architecture of the software driving the USRP NI-2901

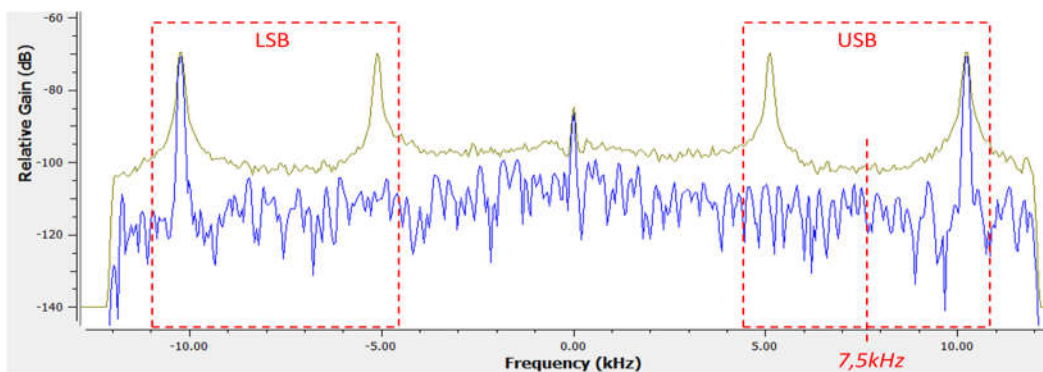


Figure 6 – Frequency spectrum of the RX signal sampled by the USRP NI-2901 in presence of the backscattered EM response from the transponder. The Figure shows the instantaneous trace in blue and the max hold trace.  
Rem: The centre frequency (0Hz) is normalized to the carrier frequency which is 3.5GHz in this case.

At the receiver side, the USRP first demodulate the incoming RX signal at the carrier frequency  $f_c$ . This step is done by the hardware frontend. Typical frequency spectrum recorded with the USRP in presence of the transponder are shown in Fig. 6. Then, the following processing is done by software. First, the IQ signals are filtered with a band-pass filter from 4kHz to 11kHz to isolate the upper side band (USB) and the lower side band (LSB) generated by the subcarrier of the backscattered signal ( $5\text{kHz} < f_{sc} < 10\text{kHz}$ ). This signal is then frequency shifted by mixing it with a sinusoid of frequency 7.5kHz to center the USB around 0Hz. A low pass filtering with a cutting frequency of 5kHz is then applied to remove the LSB component and keep only the USB. This remaining signal is then demodulated with an IQ FM demodulator. The output of this block is the baseband signal which is first decimated before being de-serialized by a decoding block. The useful data rate is close to 110 bits/s and we obtain two bytes for each transmission.

### 3 Validation

#### 3.1 Power consumption measurement

We first evaluated the power consumption of the transponder during initialization and in run stage. As shown in Fig. 7 (a), we connected a 3.3V DC voltage generator in series with a  $1\text{k}\Omega$  resistor and the transponder to perform a current measurement as a function of the time using a digital sampling oscilloscope. We can note that the initialization stage lasts 0.91s. During this stage we observe a current peak starting at  $200\mu\text{A}$  and decreasing by step until reaching  $13.9\mu\text{A}$  when entering in low power run mode. After the device passed the starting time it remains stable to a very small value of current, i.e.,  $13.9\mu\text{A}$  for 3.3V. An average value of  $8.7\mu\text{A}$  under 1.8V was measured with an ammeter (in absence of the  $1\text{k}\Omega$  series resistor). It is to be noted that during low power run stage, a frame is sent every 1.75s. Thus, the power to run the device with sensor reading and backscattering based communication in low power run is as low as  $15.66\mu\text{W}$ .

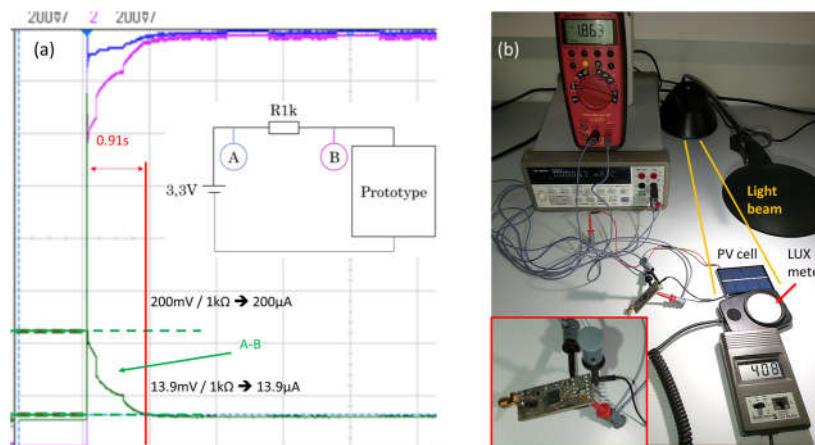


Figure 7 – (a) Current consumption measurement (b) Setup for power consumption measurement when the transponder is fed by a PV cell

#### 3.2 Empowering with a photovoltaic cell

As outlined above, the transponder requires a small amount of power to operate. Thus, it is particularly interesting to study a suitable external power supply, such a solar cell. For this study we chose a polycrystalline solar cell SOL4N of size 72mm x 46mm delivering 2V / 200mA under direct sun light ( $\sim 120\,000$  lux) but much less under overcast weather conditions (typically 2000 lux) or at sunrise / sunset (typically 400 lux). We evaluated the performance of the PV cell when directly connected to the transponder board as shown in Fig. 7(b) exposed to variable illumination condition from 500 lux to 5000 lux with the help of a desk lamp. The illuminance was controlled with a lux meter LX-101 featuring a detection spectrum in accordance with the average human vision (C.I.E. photopic). Relationship between the measured voltage and current feeding the transponder as a function of the illuminance is shown in Fig. 8 (a) and (b), respectively. One can observe a hysteresis between the rising curve (see red curve in Fig. 8 (a) and (b)) of the illuminance from the minimum (500 lux) to the maximum (5000 lux) and the falling curve (see blue curve in Fig. 8 (a) and (b)) back to the minimum. This phenomenon is explained by the initialisation stage of the microcontroller that requires much more power to start than in low power run mode.

Indeed, the microcontroller needs a voltage above 1.8V with a maximum current of 200 $\mu$ A that last 0.91s to be initialized as shown in Fig. 7 (a). In Fig. 8 (a), we observe a sharp step from 1200 $\mu$ A down to 5.6 $\mu$ A when illuminance is above 3400 lux while the voltage rises from 1.69V to 1.826V (see Fig. 8 (b)). Once the microcontroller operates in low power run, the falling curve shows that it can operate properly down to 1200 lux. These results prove that the device can be fed in outdoor environment without any storage capacity even under cloudy condition as well as in indoor environment when located close to windows in order to catch the sunlight.

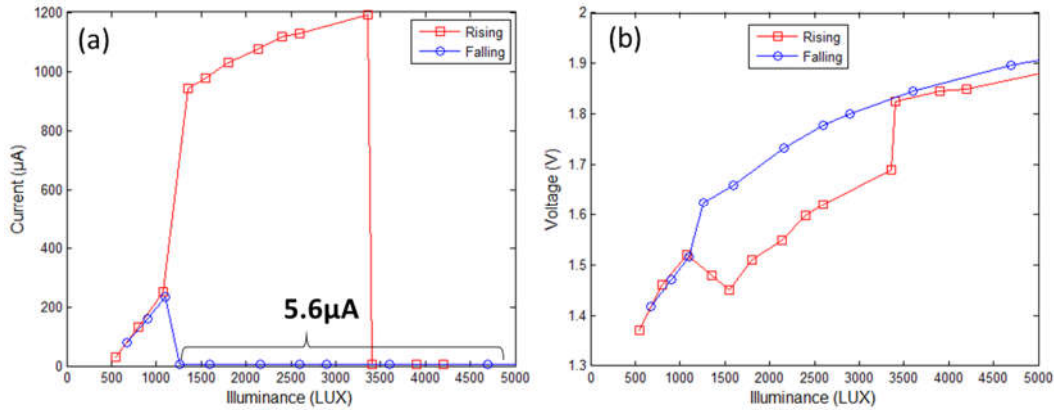


Figure 8 –Current (a) and voltage (b) fed to the transponder by a PV cell as a function of illuminance

### 3.3 Wireless communication measurements

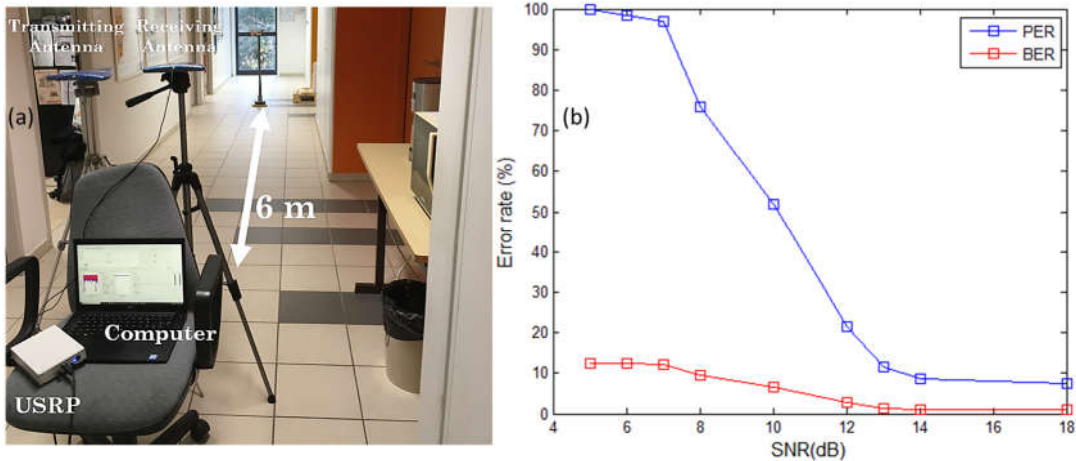


Figure 9 – (a) Measurement set-up for wireless communication testing in indoor environment (b) PER and BER as a function of SNR

The setup to test the wireless communication performance between the remote sensor and the USRP is shown in Fig. 9 (a). The testing environment is a lab corridor subjected to interferences by other radio systems and multipath, thus it is a real life scenario. The USRP NI-2901 is connected in a bistatic configuration to two wideband antennas (Aaronia Hyperlog 60100) featuring a gain close to 5dBi from 3.4GHz to 3.8GHz. As shown in the architecture diagram of Fig. 5, a continuous wave is transmitted to the TX antenna with a 20dBm of maximum output power (25dBm EIRP). It is to be noted that the receiving channel embeds an internal low noise amplifier with a gain that can be modified by software to adjust the level of demodulated IQ signals. The remote sensor is placed in front of the antenna, varying the distance to reach the maximum achievable distance measured at 6.5m for a packet error rate (PER) below 10%. This is an acceptable value because the two-bytes length data frame (temperature + humidity coded with 16 bits in this example) is permanently sent by the sensor at a refresh rate of one frame every 1.75s so that data is redundant. The measured received power with a spectrum analyzer at the location of the transponder (distance of 6.5m) is -33dBm giving a loss path of -53dB from the output port of the

USRP to the output of the receiving antenna of the remote transponder. The relationship between the measured PER and the signal to noise ratio (SNR) is given in Fig. 9 (b). A PER below 10%, giving a BER 1.4% by calculation, is achieved for a SNR above 12dB.

#### 4 Conclusion

We demonstrated the possibility to design a backscatter communication based wireless sensor operating in the 5G band from 3.4GHz to 3.8GHz. The measured average current consumption of the remote device composed of a microcontroller, a digital temperature / humidity sensor, and a SPDT switch is as low as  $8.7\mu\text{A}$  under 1.8V in low power run mode. This gives a power consumption of  $15.66\mu\text{W}$  to send a data frame permanently every 1.75s. A PV cell of size 72mm x 46mm allowed to feed the wireless sensor since an illuminance of 3400 lux when the microcontroller is first time empowered, and down to 1200 lux once initialisation stage is done. A dedicated reading system based on an USRP NI-2901 connected to two antennas in a bistatic configuration has been developed to communicate with the wireless sensor. We observe successful reading at a maximum distance of 6.5m with a PER of 10% for a radiating power of 25dBm EIRP. In a future work we will improve the decoding block of the reading system to decrease the PER for a given SNR, and we will integrate an interface block between the PV cell and the transponder to ensure operating the device under lower illuminance conditions.

#### Acknowledgments

The authors are grateful to the University of Montpellier for its support.

#### References

- [1] H. Stockman, "Communication by Means of Reflected Power," Proceedings of the I.R.E., vol. 36, pp. 1196-1204, Octobre 1948.
- [2] J. Landt, «The history of RFID,» in Proceedings of IEEE Potentials, vol. 24, pp. 8-11, 2005.
- [3] K. Finkenzeller, "RFID Handbook: Fundamentals and Applications in Contactless Smart Cards, Radio Frequency Identification and Near-field Communication," Wiley. 2010.
- [4] N. V. Huynh, D. T. Hoang, X. Lu, D. Niyato, P. Wang et D. I. Kim, «Ambient Backscatter Communications: A Contemporary Survey,» IEEE Communications Surveys & Tutorials, vol. 20, pp. 2889-2922, 2018.
- [5] S. Thomas et M. S. Reynolds, «QAM Backscatter for Passive UHF RFID Tags,» 2010 IEEE International Conference on RFID (IEEE RFID 2010), pp. 210-214, 2010.
- [6] S. N. Daskalakis, J. Kimionis, A. Collado, M. M. Tentzeris et A. Georgiadis, «Ambient FM Backscattering for Smart Agricultural Monitoring,» 2017 IEEE MTT-S International Microwave Symposium (IMS), pp. 1339-1341, Oct. 2017.
- [7] S. N. Daskalakis, J. Kimionis, A. Collado, G. Goussetis, M. M. Tentzeris et A. Georgiadis, «Ambient Backscatterers Using FM Broadcasting for Low Cost and Low Power Wireless Applications,» in IEEE Transactions on Microwave Theory and Techniques, vol. 65, pp. 5251-5262, Dec. 2017.
- [8] S. N. Daskalakis, G. Goussetis et A. Georgiadis, "Low Bitrate Ambient FM Backscattering for Low Cost and Low Power Sensing," 2018 2nd URSI Atlantic Radio Science Meeting (ATRASC), pp. 1-2, 27 September 2018.